

Mechanistic Studies on Gold-Catalyzed Direct Arene C–H Bond Functionalization by Carbene Insertion: The Coinage-Metal Effect

Manuel R. Fructos,[†] Maria Besora,[‡] Ataulpa A. C Braga,^{‡,§} M. Mar Díaz-Requejo,^{*,†} Feliu Maseras,^{*,‡,||} and Pedro J. Pérez^{*,†}

[†]Laboratorio de Catálisis Homogénea, Unidad Asociada al CSIC, CIQSO-Centro de Investigación en Química Sostenible and Departamento de Química “Prof. Jose Carlos Vilchez Martín”, Universidad de Huelva, Campus de El Carmen, 21007 Huelva, Spain

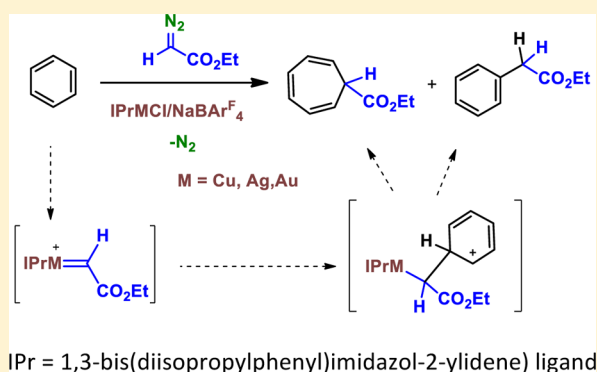
[‡]Institute of Chemical Research of Catalonia (ICIQ), The Barcelona Institute of Science and Technology, Avda. Països Catalans 16, 43007 Tarragona, Spain

[§]Departamento de Química Fundamental, Instituto de Química, Universidade de São Paulo, São Paulo, Brazil

^{||}Departament de Química, Universitat Autònoma de Barcelona, 08193 Bellaterra, Spain

S Supporting Information

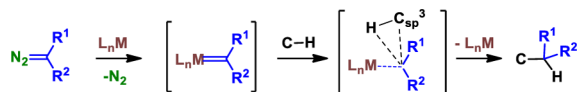
ABSTRACT: The catalytic functionalization of the C_{sp}²–H bond of benzene by means of the insertion of the CHCO₂Et group from ethyl diazoacetate (N₂=CHCO₂Et) has been studied with the series of coinage-metal complexes IPrMCl (IPr = 1,3-bis-(diisopropylphenyl)imidazol-2-ylidene) and NaBAR^F₄ (BAR^F₄ = tetrakis(3,5-bis(trifluoromethyl)phenyl)borate). For Cu and Ag, these examples constitute the first use of such metals toward this transformation, which also provides ethyl cyclohepta-2,4,6-triene-carboxylate as a byproduct from the so-called Buchner reaction. In the case of methyl-substituted benzenes, the reaction exclusively proceeds onto the aromatic ring, the C_{sp}³–H bond remaining unreacted. A significant coinage-metal effect has been observed, since the gold catalyst favors the formation of the insertion product into the C_{sp}²–H bond whereas copper and silver preferentially induce the formation of the cycloheptatriene derivative. Experimental studies and theoretical calculations have explained the observed selectivity in terms of the formation of a common Wheland intermediate, resembling an electrophilic aromatic substitution, from which the reaction pathway evolves into two separate routes to each product.



INTRODUCTION

The formation of carbon–carbon bonds is probably among the most studied processes that employ homogeneous catalysts.¹ Amid the different strategies described for such goal, a quite simple one consists of the formal insertion of a carbene CR¹R² group into a C–H bond (Scheme 1), a process that can be

Scheme 1. C_{sp}³–H Functionalization by Metal-Catalyzed Carbene Insertion from Diazo Compounds



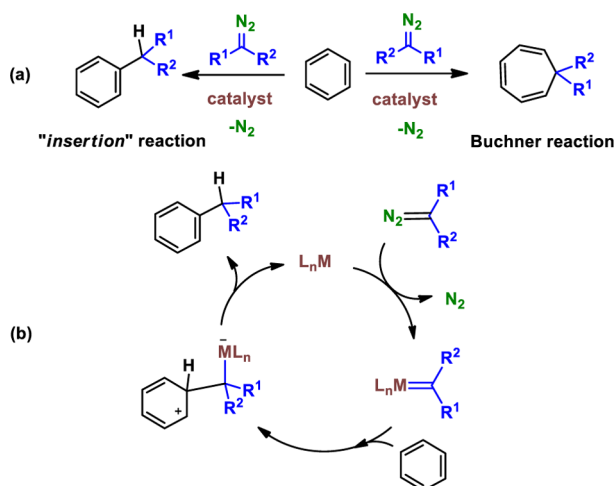
accomplished with the aid of metal-based catalysts and diazo reagents as the carbene source.^{2,3} These transformations are known to occur through the intermediacy of reactive metalcarbene intermediates,⁴ generated by extrusion of dinitrogen from the diazo molecule, which react with the hydrocarbon.

For C_{sp}³–H bonds, mechanistic studies seem to favor a concerted mechanism in which the metalcarbene carbon atom interacts with the σ C–H bond (Scheme 1). Nakamura and co-workers computed the mechanism for rhodium-based catalysts,⁵ on the basis of the previously reported experimental results,⁶ later followed by our group for the Cu- and Ag-based coinage-metal catalysts.⁷ However, the mechanistic picture is as yet unclear for the benzene (or arene) C_{sp}²–H bond functionalization with this strategy. First, this reaction competes with the so-called Buchner reaction, in which a cyclopropanation-derived norcaradiene intermediate is formed that further evolves toward a cycloheptatriene (Scheme 2a). With Rh₂(OAc)₄ as the catalyst, Shechter and Livant separately reported⁸ the metal-catalyzed functionalization of benzene by means of the *formal* insertion of the carbene unit into the C–H bond. The use of the *formal* term is related to the nature of the product obtained, but the mechanism does not seem to occur

Special Issue: Hydrocarbon Chemistry: Activation and Beyond

Received: July 27, 2016

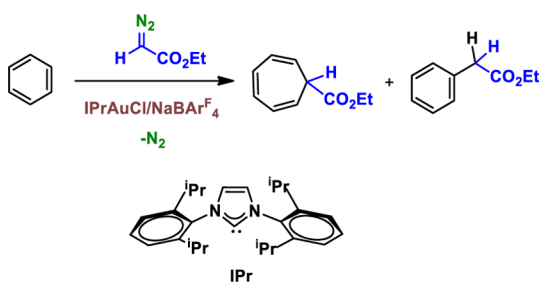
Scheme 2. (a) Arene C_{sp^2} -H Functionalization by Metal-Catalyzed Carbene Transfer from Diazo Compounds and (b) the Wheland-Based Mechanism Proposed for that Transformation



through that precise insertion pathway, at variance with the aforementioned C_{sp^3} -H bond modification. From seminal work with rhodium,^{8a,9} it was proposed that the metallocarbene originates a Wheland intermediate that undergoes a 1,2-hydrogen shift to give the final product (Scheme 2b).

Nearly a decade ago we discovered¹⁰ gold as a catalyst for the transfer of the $CHCO_2Et$ group from ethyl diazoacetate ($N_2=CHCO_2Et$, EDA), using $IPrAuCl$ (IPr = 1,3-bis-(diisopropylphenyl)imidazol-2-ylidene) to several saturated and unsaturated substrates, with $NaBAR^F_4$ (BAR^F_4 = tetrakis-(3,5-bis(trifluoromethyl)phenyl)borate) as the halide scavenger. Benzene and other alkylarenes were modified (Scheme 3), providing mixtures of the products derived from the

Scheme 3. Gold-Based Catalytic System for Carbene Transfer from Ethyl Diazoacetate and Subsequent Arene C_{sp^2} -H Functionalization



functionalization of the C_{sp^2} -H bond as well as cycloheptatrienes derived from the Buchner reaction. Interestingly, the C_{sp^3} -H bonds of the R substituents of the aromatic ring remained unreacted,¹¹ in spite of the well-known activated nature of benzylic sites. This finding paved the way to the use of this metal for carbene transfer reactions from diazo reagents.¹²

On the basis of the uncertainty of the mechanism of this C_{sp^2} -H bond functionalization, we decided to perform a mechanistic study toward that end, mixing experimental data and DFT calculations. With the series of complexes $IPrMCl$, (M = Cu, Ag, Au), we have established the influence of the metal center on the reaction outcome, from which a marked

coinage-metal effect has been found. With the support of DFT studies, a complete mechanistic picture is proposed fitting the experimental differences observed with the three metals. It is worth mentioning that a recent theoretical work by Liu, Xia, and co-workers have provided some light on this transformation on the basis of the $(PhO)_3PAu=C(Ph)CO_2Me$ species.¹³ Additionally, Hashmi and co-workers have provided interesting mechanistic studies on gold-based transformations involving vinylidene intermediates in C-H bond functionalization reactions.¹⁴

RESULTS AND DISCUSSION

Metal Effect. The series of complexes $IPrMCl$ (M = Cu, Ag, Au) have been employed as the catalyst precursor, along with 1 equiv of $NaBAR^F_4$, in the test reaction of EDA and benzene. The reactions were performed using benzene as the solvent, at room temperature, with the EDA added in one portion. The results are shown in Table 1, where a significant influence of the

Table 1. Metal Effect in the Reaction of EDA with Benzene using $IPrMCl$ + $NaBAR^F_4$ as Catalytic Precursor^a

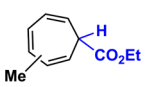
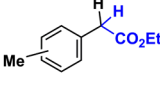
Entry	Metal	Yield ^b		
1	Cu	42 %	70 %	30 %
2	Ag	93 %	95 %	5 %
3	Au	>99 %	25 %	75 %

^aReaction conditions: catalyst loading 0.025 mmol, 0.5 mmol of EDA in 3 mL of benzene, room temperature. ^bPercentage of initial EDA converted into products as determined by NMR. The remaining initial EDA (up to 100%) was converted into diethyl fumarate and maleate.

metal center in the distribution of products has been found. Thus, the gold-based catalyst provided a regioselectivity of 75:25 favoring the alkylated product. In contrast, the silver-based catalyst only led to a very minor 5% of such product, the cycloheptatriene being by far the major products derived from benzene. The copper catalyst gave a 70:30 mixture favoring the seven-membered ring. Interestingly, the formation of diethyl fumarate and maleate as byproducts as the result of the carbene homocoupling side reaction was not observed with the gold-based catalyst, whereas both the Cu and Ag analogues led to their formation to a certain extent. Also, blank experiments carried out with pure cycloheptatriene demonstrated that under the same reaction conditions no isomerization to the insertion products was observed.¹⁵

Toluene has also been employed as the model substrate for substituted arenes containing potentially reactive C_{sp^3} -H bonds. As shown in Table 2, two different behaviors were observed. On one hand, the copper and silver catalysts predominantly led to the formation of cycloheptatrienes (88–90%), with minor amounts of the alkylated products being detected. On the other, the gold catalyst gave a mixture of both compounds, with the insertion product as the major one. A mixture of the ortho, meta, and para isomers was observed, a feature that will be commented on in the next section. It is remarkable that the product derived from the functionalization of the methyl group (that we had previously observed using copper catalysts bearing trispyrazolylborate ligands)¹⁶ was not detected in any of the three catalytic systems, supporting the

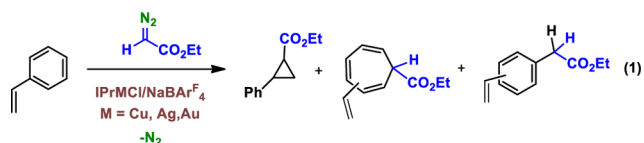
Table 2. Metal Effect in the Reaction of EDA with Toluene using $\text{IPrMCl} + \text{NaBAR}^{\text{F}}_4$ as Catalytic Precursor^a

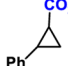
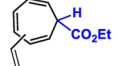
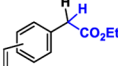
Entry	Metal	Yield ^b		
1	Cu	38 %	88 % (12:33:55) ^c	12 %
2	Ag	93 %	90 % (24:35:41) ^c	10 %
3	Au	>99 %	20 % (46:21:33) ^c	80 %

^aReaction conditions: catalyst loading 0.025 mmol, 0.5 mmol of diazo compound in 3 mL of toluene, room temperature. ^bPercentage of initial EDA converted into products as determined by NMR. The remaining initial EDA (up to 100%) was converted into diethyl fumarate and maleate. ^cOrtho:meta:para ratio.

great chemoselectivity of this $[\text{IPrM}^+]$ system toward arene functionalization over $\text{C}_{\text{sp}^3}\text{--H}$ modification.

The propensity of these catalysts to attack the arene ring has been reinforced using styrene as the substrate (eq 1 and Table

**Table 3. Metal Effect in the Reaction of EDA with Styrene using $\text{IPrMCl} + \text{NaBAR}^{\text{F}}_4$ as Catalytic Precursor^a**

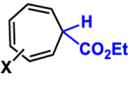
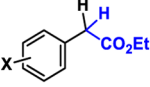
Entry	Metal	Yield ^b			
1	Cu	>99 %	88 %	7 %	4 % ^d
2	Ag	>99 %	67 %	29 %	4 % ^d
3	Au	>99 %	40 %	nd ^c	60 % ^d

^aReaction conditions: catalyst loading 0.025 mmol, 0.5 mmol of diazo compound, and 50 mmol of styrene in 3 mL of CH_2Cl_2 , room temperature. ^bPercentage of initial EDA converted into products. The remaining initial EDA (up to 100%) was converted into diethyl fumarate and maleate. ^cNot detected. ^dAs a mixture of the ortho, meta, and para isomers.

3). In addition to the expected cyclopropanes, some amounts of cycloheptatrienes and/or the insertion products are observed with the three metals. The gold catalyst provides, by far, the most significant difference, with a higher yield of the arene $\text{C}_{\text{sp}^2}\text{--H}$ functionalized product in comparison to that of cyclopropanes.

Monosubstituted Benzenes as Substrates. The use of toluene as the substrate along with the gold-based catalyst has shown a slight increase of the $\text{C}_{\text{sp}^2}\text{--H}$ functionalized product in comparison to that of benzene (80% vs 75%). We wondered about the possible effect that other substituents might exert on the selectivity. Thus, a series of monosubstituted benzenes were employed as reactants. As shown in Table 4, the nature of the

Table 4. Functionalization of Monosubstituted Benzenes with EDA in the Presence of $\text{IPrAuCl} + \text{NaBAR}^{\text{F}}_4$ ^a

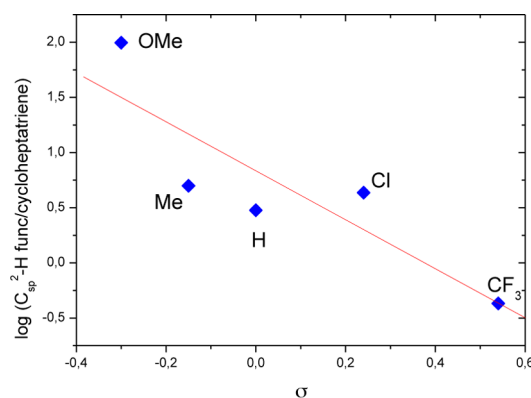
Entry	X	Yield ^b		
1	CF_3	95 %	80 % ^c (0:18:82) ^d	20 %
2	Cl	94 %	28 % ^c (41:21:38) ^d	72 %
3	H	95 %	25 % ^c	75 %
4	Me	96 %	16 % ^c (46: 21:33) ^d	80 %
5	OMe	99 %	1 % ^c (45:11:44) ^d	99 %

^aSee the Experimental Section for details. ^bPercentage of initial EDA converted into products. The remaining initial EDA (up to 100%) was converted into diethyl fumarate and maleate. ^cAs a mixture of isomers. ^dOrtho:meta:para ratio.

substituent induced a profound effect on the reaction outcome. An electron-withdrawing group such as CF_3 favored cycloheptatrienes as the major products, a situation that is reversed with electron-donating groups such as OMe. Interestingly, all $\text{C}_{\text{sp}^3}\text{--H}$ bonds remained unreacted along the series of experiments.

As mentioned above, a mixture of isomers derived from the ortho, meta, and para relative positions is observed in all cases. In an attempt to evaluate the electronic influence of the X groups in the selectivity of this transformation, a fitting of these values to the Hammett equation has been performed. For this purpose the ratio of the $\text{C}_{\text{sp}^2}\text{--H}$ functionalized and cycloheptatriene products was calculated, and its log was plotted vs σ .¹⁷

As shown in Figure 1, a good correlation with the Hammett equation is found, with a value of $\rho = -2.21 \pm 0.73$. We

**Figure 1.** Hammett σ correlation for relative rates of functionalization of monosubstituted benzene derivatives with EDA.

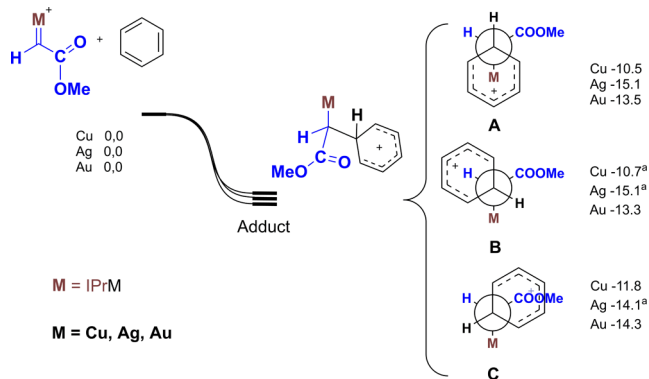
interpret this value as the result of a substantial effect of the electronic nature of the arene substituent in the distribution of products, the more donating products favoring the formal insertion reaction of the carbene group.

A competition experiment carried out with benzene and benzene- d_6 provided the following information: (i) the amounts of the products derived from both arenes were nearly identical within experimental error and (ii) kinetic experiments on nitrogen evolution gave also identical curves in both cases (see Figure S1 in Supporting Information). From these data we can conclude that the rate-determining step is located much earlier than the C–H cleavage (probably the metallocarbene formation).

All experimental evidence collected in this and previous work seems to support a pathway which differs from that of the C_{sp^3} –H bonds (Scheme 1). At variance with that metallocarbene C–H bond one-step interaction, the C_{sp^2} –H bond functionalization with this strategy displays features resembling an aromatic electrophilic substitution. In order to find additional support for such an alternative, we have carried out DFT studies that not only must provide the reaction pathway but also explain the selectivities observed regarding the effect of the metal in the chemoselectivity (insertion vs addition products).

DFT Studies. We have computationally investigated the reaction mechanisms for the reaction between the metallocarbene $IPrM=C(H)COOMe$ and benzene ($M = Cu, Ag, Au$) in order to explain the different insertion/addition ratios experimentally observed. The initial approach between the metallocarbene and benzene leads to the formation of an adduct with a new C–C bond (distance below 1.66 Å) between the carbenic carbon and benzene (Scheme 4). This adduct,

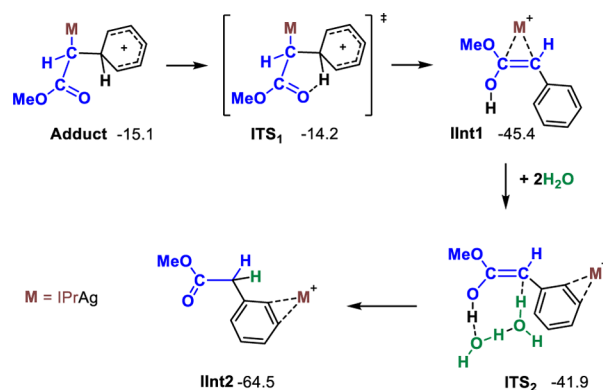
Scheme 4. Reaction of the Metallocarbene and Benzene to Form the Wheland Intermediate and Fischer Projection of the Three Main Conformers of this Intermediate^a



which is reached without any barrier in the potential energy surface, may be viewed as a Wheland intermediate. Three conformers (A, B, and C) of the adduct are in principle accessible depending on the relative orientation of substituents with respect to the newly formed C–C bond (see Scheme 4).

The adducts can evolve toward either insertion or addition products. Scheme 5 shows such evolution for the insertion pathway for the particular case of conformer A of the silver species. It starts with a proton transfer to the oxygen of the carbonyl to form an enol intermediate (ITS1). The enol IInt1 assisted by two water molecules or another enol molecule performs a keto–enol rearrangement (ITS2) to transfer the hydrogen from the oxygen to the former carbenic carbon, affording the final alkylated (“insertion”) product IInt2. An analogous mechanism of insertion has been recently postulated for a similar gold system.¹³ The proton transfer to a carbonyl

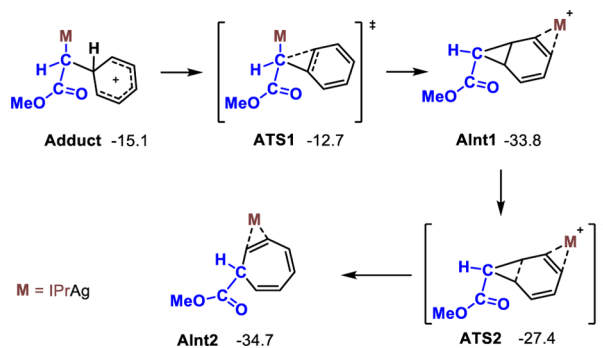
Scheme 5. Postulated Mechanism for the Insertion Reaction from Adduct A in the Case of Ag^a



compound is now a well-known feature of many metal carbene transformations of diazocarbonyl compounds.^{18,19} The contribution of water in the long distance proton transfers has been proposed even for a protodeauration step.²⁰

The Buchner reaction (addition) pathway is summarized in Scheme 6. First, a second C–C bond is made through

Scheme 6. Postulated Mechanism for the Buchner Reaction from Adduct A in the Case of Ag



transition state ATS1. In most cases, ATS1 evolves directly to AInt1, where the metal coordinates to the aromatic ring. Finally, the AInt1 undergoes an electrocyclic opening (ATS2) to form the cycloheptatriene AInt2, the addition final product. There is certainly no experimental evidence concerning the π complexes we propose in this mechanism, but we assume they are correct because of the overall agreement between computational results and experiment. The proposed mechanism is moreover in agreement with that previously reported for the Echavarren (retro-Buchner) reaction, a gold-catalyzed decarbenation (carbene extrusion from cycloheptatriene) process.²¹ Schemes 5 and 6 correspond to the Ag species, but the results are similar for the Cu and Au complexes. Some minor differences exist, however; for instance, in the case of Au, the final intermediates are better described as η^1 complexes rather than metallacyclopropenes.

In most computational mechanistic studies, the predicted product ratio could be obtained directly by comparing the barriers associated with the competing transition states ITS1 and ATS1. However, the combined presence of the three possible conformations for the adduct and its association to

very shallow minima with at least two exit channels lead to a rather more complicated picture. The importance of conformers into the study of reaction mechanisms has been previously acknowledged.²² The complexity of the picture can first be seen in Table 5. Here we attempt to collect the free

Table 5. Relative Free Energies (kcal/mol) of the Key Minima and Transition States for the Addition/Insertion Pathways

metal	A	B	C
Cu			
	adduct	−10.5	−10.7 ^a
	ATS1	−8.4 ^a	−13.4 ^a
	ITS1	−10.0	−10.0
Ag			
	adduct	−15.1	−15.1 ^a
	ATS1	−12.7	−17.1 ^a
	ITS1	−14.2	−14.2
Au			
	adduct	−13.5	−13.3
	ATS1	−8.5	−8.1
	ATS2	−7.0	−7.0
	ITS1	−12.2	−12.2

^aEnergies corresponding to structures optimized with a frozen parameter.

energies of the key points for each metal complex and each conformation. Not all points could be located as stationary points, and we had to carry out constrained geometry optimizations (freezing selected distances, structures marked with the superscript *a*) to estimate their energies. This has minor implications for some structures, such as ATS1 for Cu, which has a higher energy than both the corresponding adduct and ITS1 and likely means that in this case insertion is not feasible. However, it is critical in other cases such as the B conformers for both Cu and Ag. In this case, there is no stationary point associated with the adduct and the constrained transition state ATS1 has a lower energy than the adduct. The straightforward interpretation is that in the complex-benzene approach corresponding to conformation B there is a direct path from the separated reactants to the Alnt1 species.

Direct application of transition state theory to the results in Table 5 would predict 100% of addition product for Cu and Ag, as a barrierless process should be always preferred. In the case of gold, insertion should be preferred also at nearly 100% proportion, as the free energy differences between the competing transition states are larger than 4 kcal/mol. The experimental trend of addition (Bucher reaction) being favored for copper and silver and insertion being favored for gold is reproduced. However, the experimental ratios, with the major product never being above 90%, are definitely not reproduced. This is a serious disagreement between calculations and experiment that throws into question the validity of our computational analysis. In order to justify the validity of the calculations, we have analyzed the validity of the underlying computational approaches, and we provide below a qualitative justification of the discrepancy. We think that the origin of the discrepancy is in the limitations of the transition state theory (TST), which does not apply properly to this situation.²³ TST assumes redistribution of internal energy among the vibrational modes and internal rotations previous to any reaction step. This is not always the case, as has been recently shown in cases with

shallow intermediates and an excess of total energy.^{24–26} It is possible that in our system, once the adduct is formed, the subsequent step takes place before the energy redistribution occurs.

To explore this, we have conducted Born–Oppenheimer molecular dynamics (BOMD) calculations²⁷ on the simplified model of our system of interest: NHC-M=CH(COOH) + C₆H₆. This type of quantum dynamics has been previously used with success.²⁸ We centered our attention to the first part of the reaction where the first C–C bond is formed with the immediate evolution of this unstable intermediate toward one of the products. We ran only 10 trajectories for each approach and metal, a total of 90 trajectories.

The results of the BOMD calculations are summarized in Table 6. We have counted the number of trajectories going

Table 6. Number of Trajectories Going through the Addition/Insertion/Nonreactive Reaction Pathways, Depending on the Metal Center (Cu, Ag, Au) and the Considered Conformer (A, B, C)

metal	A	B	C
Cu	9/0/1	8/2/0	6/0/4
Ag	8/0/2	6/3/1	5/0/5
Au	0/0/10	0/8/2	0/0/10

through addition/insertion/nonreactive reaction pathways. In the trajectories labeled as nonreactive, the complex remains as a Wheland intermediate or forms unstable intermediates that are expected to revert to it. For the copper catalyst 23 of the 25 productive trajectories lead to the addition product and 2 of them, all associated with path B, to the insertion product. The case of silver is similar, with 19 out of 22 going to addition and 3 out of 22 leading to insertion. We note that for copper 23:2 would mean a proportion of 92:8 and for silver 19:3 translates to 86:14. The numbers are reasonably close to the experimental observations of 70:30 and 95:5, respectively. There are at least two major problems in the translation of reacting trajectories to total ratios: namely, the small number of trajectories and the assumption that the three paths have an identical probability. Therefore, we do not claim this as an accurate prediction. However, we consider these results indicative that extensions beyond transition state theory do improve the agreement with experiment in this system. We finally admit that these results can still not explain the experimentally reported 25:75 result in the gold system, as calculations still suggest 0:100. Explanation of this result may require a more accurate dynamic study, which is out of the scope of the current work.

The calculations reported above show an unexpected complexity in the system but can yet provide a reasonable reproduction of the experimental results. The key to the different behavior of the gold complex lies in the energetics of addition for path B. The step is barrierless in the potential energy surface for copper and silver but has a barrier of 5.2 kcal/mol for gold. The higher barrier may be associated with the existence of a substrate rearrangement in the metal coordination sphere along this pathway, which is a poor fit for the limited stability of Au(I) compounds with coordination numbers above 2.

CONCLUSIONS

In summary, we have found that the catalytic system formed by complexes IPrMCl and NaBAR₄^F (M = Cu, Ag, Au; IPr = 1,3-

bis(diisopropylphenyl)imidazol-2-ylidene; BAr_4^{F} = tetrakis(3,5-bis(trifluoromethyl)phenyl)borate), benzene, and ethyl diazoacetate promotes the functionalization of the aromatic ring, providing mixtures of products derived from direct $\text{C}_{\text{sp}^2}\text{--H}$ bond modification as well as cycloheptatriene rings derived from the Buchner reaction. The selectivity strongly depends on the nature of the coinage metal: Cu and Ag favored ethyl cycloheptatriene-1-carboxylate, whereas gold gave the alkylated arene as the major product. With toluene as the substrate, a similar behavior is observed, although the methyl group remained unreacted, as a consequence of a high selectivity toward the arene vs aliphatic C--H bond. Experimental data and DFT calculations support the existence of a mechanistic pathway in which a Wheland-type intermediate is first formed, from which two alternative routes might occur. That of the insertion product resembles the aromatic electrophilic substitution, at variance with the concerted, one-step mechanistic view of the functionalization of $\text{C}_{\text{sp}^3}\text{--H}$ by carbene insertion.

EXPERIMENTAL SECTION

General Methods. All reactions were carried out under an oxygen-free nitrogen atmosphere by using an MBraun-Unilab glovebox containing dry argon or nitrogen or conventional Schlenk techniques. Solvents were purchased from Aldrich and were rigorously dried before use. The reagents were also purchased from Aldrich and were employed without further purification. The complexes IPrMCl and $\text{NaBAr}_4^{\text{F}}$ were prepared according to the literature.^{29,30} NMR solvents were stored over molecular sieves under nitrogen. NMR spectra were measured on Agilent 400 MR and 500 DD2 spectrometers. GC data were collected with a Varian GC-3900 spectrometer with an FID detector.

General Catalytic Experiment. The precatalyst IPrMCl (0.025 mmol) was dissolved in 3 mL of the corresponding substrate, and $\text{NaBAr}_4^{\text{F}}$ (0.025 mmol) was added to the solution. After 15 min, EDA (0.5 mmol) was added in one portion. After it was stirred at room temperature for 72 h, the mixture was analyzed by GC and GCMS. The volatiles were removed under reduced pressure, and the residue was analyzed by NMR spectroscopy to identify the products. See the [Supporting Information](#) for experimental details.

Computational Details. The DFT studies presented have been performed with Grimme's B97D³¹ functional including a D2 empirical dispersion correction as implemented in Gaussian 09.³² 6-31g(d) basis sets³³ were used for all atoms except for the three metals of the catalysts (Cu, Ag, and Au) for which lanl2dz³⁴ was used instead together with the corresponding ECP and an additional polarization function f with the exponents Cu ($\zeta(f) = 3.525$), Ag ($\zeta(f) = 1.611$), and Au ($\zeta(f) = 1.050$).³⁵ Solvent effects have been taken into account through the continuum model SMD for benzene.³⁶ The model used was the same metallocarbene used experimentally except for the ethyl group of the COOEt , which was replaced by a methyl. The static calculations presented correspond to minima or transition states as confirmed by frequency calculations; however, due to the particularities of the considered potential energy surface some of the structures presented correspond to geometries with a frozen distance between atoms. These energies should only be taken as orientative and are marked with an F in the schemes and text. All energies presented correspond to free energies in solution and are given in kcal/mol.

To achieve a better understanding of the reactivity of the system, quantum dynamics under the Born–Oppenheimer molecular dynamics (BOMD) model²⁷ as implemented in Gaussian 09³⁷ were carried out. The system was simplified by pruning the diisopropylphenyl groups of the metallocarbene IPr to hydrogens and the ethyl group of the carbene also to hydrogen. The dynamics calculations were initiated from geometries where the carbenic carbon and one of the carbons of the benzene were set to 2.5 Å and the rest of the molecule was optimized, as a calculation from the separate reactants would be unfeasible in terms of computational effort. The initial

kinetic energy was taken as the difference between the starting point and the separate reactants in the potential energy surface, and the initial velocities were obtained from a preliminary calculation with the `nsample` keyword and provision of the mode number and vibrational energy corresponding to the mode for the stretch between the carbenic carbon and the closest carbon of the benzene. The calculations were performed defining the phase for the transition vector between the carbonic carbon and one of the benzene carbons, for a rotational temperature of 300 K, performing Hessian updates every 12 gradient points before doing a new analytic Hessian. For each system 10 trajectories were considered reading in initial velocities. For the more reactive Ag we performed 3000 steps which correspond to approximately 2 ps. For Cu and Au we generated 6000 steps corresponding to approximately 4 ps; some tests with 12000 steps were run for selected systems.

A data set collection of computational results is available in the IoChem-BD repository³⁸ and can be accessed via <http://dx.doi.org/10.19061/iochem-bd-1-11>.

ASSOCIATED CONTENT

Supporting Information

The Supporting Information is available free of charge on the ACS Publications website at DOI: 10.1021/acs.organomet.6b00604.

Detailed experimental catalytic and mechanistic procedures, including kinetic isotopic effect studies and computational data including transition states geometries and Cartesian coordinates and energies of all stationary points reported in the text (PDF)

Cartesian coordinates of calculated structures (XYZ)

AUTHOR INFORMATION

Corresponding Authors

*E-mail for M.M.D.-R.: mmdiaz@dqcm.uhu.es.

*E-mail for F.M.: fmaseras@iciq.es.

*E-mail for P.J.P.: perez@dqcm.uhu.es.

Notes

The authors declare no competing financial interest.

ACKNOWLEDGMENTS

We thank the Spanish MINECO for CTQ2014-52769-C3-1-R, CTQ2014-57761-R, RED INTECAT CTQ2014-52974-REDC and Severo Ochoa Excellence Accreditation 2014-2018 SEV-2013-0319 and the ICIQ Foundation for financial support.

REFERENCES

- (1) Hartwig, J. F. *Organotransition Metal Chemistry: From Bonding to Catalysis*; University Science Books: Sausalito, CA, 2010.
- (2) (a) Doyle, M. P.; Duffy, R.; Ratnikov, M.; Zhou, L. *Chem. Rev.* **2010**, *110*, 704–724. (b) Doyle, M. P.; McKervey, M. A.; Ye, T. *Modern Catalytic Methods for Organic Synthesis with Diazo Compounds*; Wiley: New York, 1998. (c) Davies, H. M. L.; Dick, A. R. *Top. Curr. Chem.* **2009**, *292*, 303–345. (d) Davies, H. M. L.; Manning, J. R. *Nature* **2008**, *451*, 417–424.
- (3) (a) Caballero, A.; Díaz-Requejo, M. M.; Frutos, M. R.; Olmos, A.; Urbano, J.; Pérez, P. J. *Dalton Trans.* **2015**, *44*, 20295–20307. (b) Díaz-Requejo, M. M.; Pérez, P. J. *Chem. Rev.* **2008**, *108*, 3379–3394. (c) Díaz-Requejo, M. M.; Belderráin, T. R.; Nicasio, M. C.; Pérez, P. J. *Dalton Trans.* **2006**, 5559–5566.
- (4) Examples of metallocarbene species from diazo reagents: (a) Werlé, C.; Goddard, R.; Philipps, P.; Farès, C.; Fürstner, A. J. *Am. Chem. Soc.* **2016**, *138*, 3797–3805. (b) Werlé, C.; Goddard, R.; Fürstner, A. *Angew. Chem., Int. Ed.* **2015**, *54*, 15452–15456. (c) Hussong, M. W.; Hoffmeister, W. T.; Rominger, F.; Straub, B. *Angew. Chem., Int. Ed.* **2015**, *54*, 10331–10335. (d) Hussong, M.

- W.; Rominger, F.; Krämer, P.; Straub, B. F. *Angew. Chem., Int. Ed.* **2014**, *53*, 9372–9375. (e) Pereira, A.; Champouret, Y.; Martín, C.; Álvarez, E.; Etienne, M.; Belderrain, T. R.; Pérez, P. J. *Chem. - Eur. J.* **2015**, *21*, 9769–9775. (f) Kornecki, K. P.; Briones, J. F.; Boyarskikh, V.; Fullilove, F.; Autschbach, J.; Schrote, K. E.; Lancaster, K. M.; Davies, H. M. L.; Berry, J. F. *Science* **2013**, *342*, 351–354. (g) Chattopadhyay, P.; Matsuo, T.; Tsuji, T.; Ohbayashi, J.; Hayashi, T. *Organometallics* **2011**, *30*, 1869–1873. (h) Russell, S. K.; Lobkovsky, E.; Chirik, P. J. *J. Am. Chem. Soc.* **2009**, *131*, 36–37. (i) Deng, Q.-H.; Chen, J.; Huang, J.-S.; Chui, S. S.-Y.; Zhu, N.; Li, G.-Y.; Che, C.-M. *Chem. - Eur. J.* **2009**, *15*, 10707–10712. (j) Mankad, N. P.; Peters, J. C. *Chem. Commun.* **2008**, 1061–1063. (k) Dai, X. L.; Warren, T. H. *J. Am. Chem. Soc.* **2004**, *126*, 10085–10094. (l) Straub, B. F.; Hofmann, P. *Angew. Chem., Int. Ed.* **2001**, *40*, 1288–1290.
- (5) Nakamura, E.; Yoshikai, N.; Yamanaka, M. *J. Am. Chem. Soc.* **2002**, *124*, 7181–7192.
- (6) For a comprehensive review on diazo-carbonyls in organic synthesis including C–H functionalization see: (a) Ye, T.; McKervy, M. A. *Chem. Rev.* **1994**, *94*, 1091–1160. (b) Ford, A.; Miel, H.; Ring, A.; Slaterry, C. N.; Maguire, A. R.; McKervy, M. A. *Chem. Rev.* **2015**, *115*, 9981–10080.
- (7) Braga, A. A. C.; Maseras, F.; Urbano, J.; Caballero, A.; Díaz-Requejo, M. M.; Pérez, P. J. *Organometallics* **2006**, *25*, 5292–5300.
- (8) (a) Rosenfeld, M. J.; Shankar, B. K.; Shechter, H. J. *Org. Chem.* **1988**, *53*, 2699–2705. (b) Yang, M.; Webb, T. R.; Livant, P. J. *Org. Chem.* **2001**, *66*, 4945–4949.
- (9) Padwa, A.; Austin, D. J.; Price, A. T.; Semones, M. A.; Doyle, M. P.; Protopopova, M. N.; Winchester, W. R.; Tarn, A. J. *Am. Chem. Soc.* **1993**, *115*, 8669–8680.
- (10) Frutos, M. R.; Belderrain, T. R.; Frémont, P.; Scott, N. M.; Nolan, S. P.; Díaz-Requejo, M. M.; Pérez, P. J. *Angew. Chem., Int. Ed.* **2005**, *44*, 5284–5288.
- (11) (a) Rivilla, I.; Gómez-Emeterio, B. P.; Frutos, M. R.; Díaz-Requejo, M. M.; Pérez, P. J. *Organometallics* **2011**, *30*, 2855–2860. (b) Pérez, P. J.; Díaz-Requejo, M. M.; Rivilla, I. *Beilstein J. Org. Chem.* **2011**, *7*, 653–657.
- (12) Frutos, M. R.; Díaz-Requejo, M. M.; Pérez, P. J. *Chem. Commun.* **2016**, 52, 7326–7335.
- (13) Liu, Y.; Yu, Z.; Luo, Z.-L.; Zhang, J. Z.; Liu, L.; Xia, F. J. *Phys. Chem. A* **2016**, *120*, 1925–1932.
- (14) (a) Vilhelmsen, M. H.; Hashmi, A. S. K. *Chem. - Eur. J.* **2014**, *20*, 1901–1908. (b) Hashmi, A. S. K. *Acc. Chem. Res.* **2014**, *47*, 864–876.
- (15) For such acid-catalyzed isomerization see: McKervy, M. A.; Russell, D. N.; Twohig, M. F. *J. Chem. Soc., Chem. Commun.* **1985**, 491–492.
- (16) Morilla, M. E.; Díaz-Requejo, M. M.; Belderrain, T. R.; Nicasio, M. C.; Trofimenko, S.; Pérez, P. J. *Organometallics* **2004**, *23*, 293–295.
- (17) March, J. *Advanced Organic Chemistry, Reactions, Mechanisms and Structure*, 7th ed.; Wiley-Interscience: New York, 2013.
- (18) (a) Ma, B.; Wu, Z.; Huang, B.; Liu, L.; Zhang, J. L. *Chem. Commun.* **2016**, 52, 9351–9354. (b) Liu, H.; Duan, J.-X.; Qu, D.; Guo, L.-P.; Xie, Z.-Z. *Organometallics* **2016**, *35*, 2003–2009. (c) Xie, Q.; Song, X.-S.; Qu, D.; Guo, L.-P.; Xie, Z.-Z. *Organometallics* **2015**, *34*, 3112–3119. (d) Xie, Z.-Z.; Liao, W.-J.; Cao, J.; Guo, L. P.; Verpoort, F.; Fang, W. *Organometallics* **2014**, *33*, 2448–2456. (e) Moniz, G. A.; Wood, J. L. *J. Am. Chem. Soc.* **2001**, *123*, 5095–5097. (f) Wood, J. L.; Moniz, G. A. *Org. Lett.* **1999**, *1*, 371–374.
- (19) (a) Zhang, D.; Zhou, J.; Xia, F.; Kang, Z.; Hu, W. *Nat. Commun.* **2015**, *6*, 5801–5808. (b) Qiu, H.; Li, M.; Jiang, L.-Q.; Lv, F. P.; Zan, Li; Zhai, C. W.; Doyle, M. P.; Hu, W.-H. *Nat. Chem.* **2012**, *4*, 733–738.
- (20) Krauter, C. M.; Hashmi, A. S. K.; Pernpointner, M. *ChemCatChem* **2010**, *2*, 1226–1230.
- (21) Wang, Y.; McGonigal, P. R.; Herlé, B.; Besora, M.; Echavarren, A. M. *J. Am. Chem. Soc.* **2014**, *136*, 801–809.
- (22) Besora, M.; Braga, A. A. C.; Ujaque, G.; Maseras, F.; Lledós, A. *Theor. Chem. Acc.* **2011**, *128*, 639–646.
- (23) Truhlar, D. G.; Garrett, B. C.; Klippenstein, S. J. *J. Phys. Chem.* **1996**, *100*, 12771–12800.
- (24) (a) Reyes, M. B.; Carpenter, B. K. *J. Am. Chem. Soc.* **2000**, *122*, 10163–10176. (b) Carpenter, B. K. *Annu. Rev. Phys. Chem.* **2005**, *56*, 57–89. (c) Carpenter, B. K. *Chem. Rev.* **2013**, *113*, 7265–7286. (d) Carpenter, B. K.; Harvey, J. N.; Orr-Ewing, A. J. *J. Am. Chem. Soc.* **2016**, *138*, 4695–4705.
- (25) (a) Litovitz, A. E.; Keresztes, I.; Carpenter, B. K. *J. Am. Chem. Soc.* **2008**, *130*, 12085–12094. (b) Xu, L.; Doubleday, C. E.; Houk, K. N. *J. Am. Chem. Soc.* **2011**, *133*, 17848–17854.
- (26) (a) Doubleday, C.; Li, G.; Hase, W. L. *Phys. Chem. Chem. Phys.* **2002**, *4*, 304–312. (b) Singleton, D. A.; Hang, C.; Szymanski, M. J.; Meyer, M. P.; Leach, A. G.; Kuwata, K. T.; Chen, J. S.; Greer, A.; Foote, C. S.; Houk, K. N. *J. Am. Chem. Soc.* **2003**, *125*, 1319–1328. (c) Bekele, T.; Christian, C. F.; Lipton, M. A.; Singleton, D. A. *J. Am. Chem. Soc.* **2005**, *127*, 9216–9223. (d) Doubleday, C.; Suhrada, C. P.; Houk, K. N. *J. Am. Chem. Soc.* **2006**, *128*, 90–94. (e) Bach, A.; Hostettler, J. M.; Chen, P. J. *Chem. Phys.* **2006**, *125*, 024304. (f) Schmittel, M.; Vavilala, C.; Jaquet, R. *Angew. Chem., Int. Ed.* **2007**, *46*, 6911–6914. (g) Hamaguchi, M.; Nakaishi, M.; Nagai, T.; Nakamura, T.; Abe, M. *J. Am. Chem. Soc.* **2007**, *129*, 12981–12988. (h) Oyola, Y.; Singleton, D. A. *J. Am. Chem. Soc.* **2009**, *131*, 3130–3131. (i) Wang, Z.; Hirschi, J. S.; Singleton, D. A. *Angew. Chem., Int. Ed.* **2009**, *48*, 9156–9159. (j) Quijano, L. M. M.; Singleton, D. A. *J. Am. Chem. Soc.* **2011**, *133*, 13824–13824. (k) Patel, A.; Chen, Z.; Yang, Z.; Gutiérrez, O.; Liu, H.; Houk, K. N.; Singleton, D. A. *J. Am. Chem. Soc.* **2016**, *138*, 3631–3634.
- (27) (a) Helgaker, T.; Uggerud, E.; Jensen, H. J. A. *Chem. Phys. Lett.* **1990**, *173*, 145–274. (b) Uggerud, E.; Helgaker, T. *J. Am. Chem. Soc.* **1992**, *114*, 4265–4268.
- (28) (a) Xu, L.; Doubleday, C. E.; Houk, K. N. *J. Am. Chem. Soc.* **2011**, *133*, 17848–17854. (b) Black, K.; Liu, P.; Xu, L.; Doubleday, C.; Houk, K. N. *Proc. Natl. Acad. Sci. U. S. A.* **2012**, *109*, 12860–12865.
- (29) (a) de Fremont, P.; Scott, N. M.; Stevens, E. D.; Nolan, S. P. *Organometallics* **2005**, *24*, 2411–2418. (b) Jurkauskas, V.; Sadighi, J. P.; Buchwald, S. L. *Org. Lett.* **2003**, *5*, 2417–2420. (c) de Fremont, P.; Scott, N. M.; Stevens, E. D.; Ramnial, T.; Lightbody, O. C.; MacDonald, C. L. B.; Clyburne, A. C.; Abernethy, C. D.; Nolan, S. P. *Organometallics* **2005**, *24*, 6301–6309.
- (30) (a) Brookhart, M.; Grant, B.; Volpe, A. F. *Organometallics* **1992**, *11*, 3920–3922. (b) Iwamoto, H.; Sonoda, T.; Kobayashi, H. *Tetrahedron Lett.* **1983**, *24*, 4703–4706.
- (31) Grimme, S. *J. Comput. Chem.* **2006**, *27*, 1787–1799.
- (32) Frisch, M. J.; Trucks, G. W.; Schlegel, H. B.; Scuseria, G. E.; Robb, M. A.; Cheeseman, J. R.; Scalmani, G.; Barone, V.; Mennucci, B.; Petersson, G. A.; Nakatsuji, H.; Caricato, M.; Li, X.; Hratchian, H. P.; Izmaylov, A. F.; Bloino, J.; Zheng, G.; Sonnenberg, J. L.; Hada, M.; Ehara, M.; Toyota, K.; Fukuda, R.; Hasegawa, J.; Ishida, M.; Nakajima, T.; Honda, Y.; Kitao, O.; Nakai, H.; Vreven, T.; Montgomery, J. A., Jr.; Peralta, J. E.; Ogliaro, F.; Bearpark, M.; Heyd, J. J.; Brothers, E.; Kudin, K. N.; Staroverov, V. N.; Kobayashi, R.; Normand, J.; Raghavachari, K.; Rendell, A.; Burant, J. C.; Iyengar, S. S.; Tomasi, J.; Cossi, M.; Rega, N.; Millam, J. M.; Klene, M.; Knox, J. E.; Cross, J. B.; Bakken, V.; Adamo, C.; Jaramillo, J.; Gomperts, R.; Stratmann, R. E.; Yazyev, O.; Austin, A. J.; Cammi, R.; Pomelli, C.; Ochterski, J. W.; Martin, R. L.; Morokuma, K.; Zakrzewski, V. G.; Voth, G. A.; Salvador, P.; Dannenberg, J. J.; Dapprich, S.; Daniels, A. D.; Farkas, Ö.; Foresman, J. B.; Ortiz, J. V.; Cioslowski, J.; Fox, D. J. *Gaussian 09, Revision D.01*; Gaussian, Inc., Wallingford, CT, 2009.
- (33) (a) Hehre, W. J.; Ditchfield, R.; Pople, J. A. *J. Chem. Phys.* **1972**, *56*, 2257–2261. (b) Hariharan, P. C.; Pople, J. A. *Theor. Chem. Acc.* **1973**, *28*, 213–222.
- (34) (a) Hay, P. J.; Wadt, W. R. *J. Chem. Phys.* **1985**, *82*, 270–283. (b) Hay, P. J.; Wadt, W. R. *J. Chem. Phys.* **1985**, *82*, 299–310.
- (35) Ehlers, A. W.; Böhme, M.; Dapprich, S.; Gobbi, A.; Höllwarth, A.; Jonas, V.; Köhler, K. F.; Stegmann, R.; Veldkamp, A.; Frenking, G. *Chem. Phys. Lett.* **1993**, *208*, 111–208.
- (36) Marenich, A. V.; Cramer, C. J.; Truhlar, D. G. *J. Phys. Chem. B* **2009**, *113*, 6378–6396.
- (37) (a) Chen, W.; Hase, W. L.; Schlegel, H. B. *Chem. Phys. Lett.* **1994**, *228*, 436–442. (b) Millam, J. M.; Bakken, V.; Chen, W.; Hase,

W. L.; Schlegel, H. B. *J. Chem. Phys.* **1999**, *111*, 3800–3805. (c) Li, X.; Millam, J. M.; Schlegel, H. B. *J. Chem. Phys.* **2000**, *113*, 10062–10067.
(38) Álvarez-Moreno, M.; de Graaf, C.; López, N.; Maseras, F.; Poblet, J. M.; Bo, C. *J. Chem. Inf. Model.* **2015**, *55*, 95–103.